Chemical Engineering Journal 366 (2019) 112–122

Contents lists available at ScienceDirect

Chemical Engineering Journal

journal homepage: www.elsevier.com/locate/cej

Directly photopatterning of polycaprolactone-derived photocured resin by UV-initiated thiol-ene "click" reaction: Enhanced mechanical property and excellent biocompatibility

Yazhi Zhu[a,1], Jian Shen[b,1], Li Yin[b,1], Xiaojuan Wei[a], Feng Chen[a,*], Mingqiang Zhong[a], Zheng Gu[b], Yao Xie[b,*], Wei Jin[b], Zhenjie Liu[b,*], Chandani Chitrakar[c], Lingqian Chang[d,e]

[a] College of Chemical Engineering and Materials Science, Zhejiang University of Technology, Hangzhou 310014, PR China
[b] Second Affiliated Hospital of Zhejiang University School of Medicine, Hangzhou 310009, PR China
[c] Department of Biomaterial Engineering, University of North Texas, Denton, TX 76207, USA
[d] School of Biological Science and Medical Engineering, Beihang University, Beijing 10083, PR China
[e] Institute of nanotechnology for Single Cell Analysis (INSCA), Beijing Advanced Innovation Center for Biomedical Engineering, Beihang University, Beijing 10083, PR China

HIGHLIGHTS

- We report a photocured resin with enhanced mechanical property and excellent biocompatibility.
- The resin can be photocured via UV through thiol-ene "click" chemistry.
- We show the facile fabrication of high-resolution patterns (~5 μm) using photolithography.
- The technology is simple, versatile and has potential in bioengineering field.

GRAPHICAL ABSTRACT

In order to achieve a photocured resin with enhanced mechanical property and excellent biocompatibility, we have investigated a PCL-derived photocured material via UV through thiol-ene "click" chemistry and this facile route for fabrication of high-resolution patterns (~5 μm) has a good impact in bioengineering and biomedical fields.

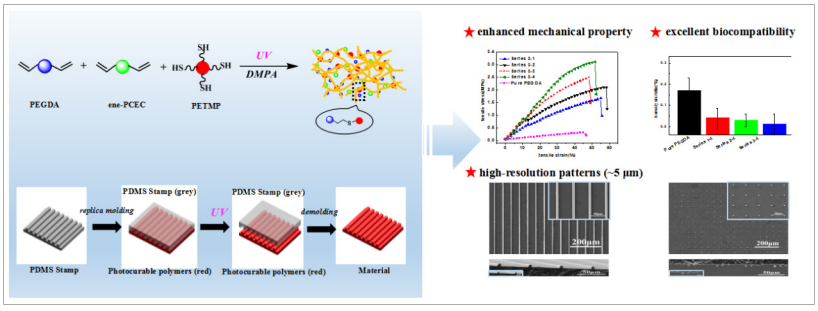

ARTICLE INFO

Keywords:
Photopatterning
Click reaction
PCL
Mechanical property
Biocompatibility

ABSTRACT

This paper reports a novel routine for the fabrication of a polycaprolactone-derived (PCL-derived) photocured material cross-linked by pentaerythritol tetra (PETMP) with enhanced mechanical property and excellent biocompatibility. The photocured material is cross-linked *via* UV irradiation through thiol-ene "click" chemistry. The main novelty of this technique is the facile fabrication of high-resolution patterns (~5 μm) using photolithography, and without adding photo-initiators. The photocured material is studied regarding to its thermal property, mechanical property and cytocompatibility. DSC and DMA suggest that the flexibility and toughness of PCL-derived photocured material have improved. Accordingly, the PCL-derived photocured material achieves enhanced mechanical property (with the increase of PCL segment content from 0 to 38.0%, the photocured samples monotonically increased their breaking strength from 0.62 to 3.10 MPa and Young's modulus from 1.39

* Corresponding authors at: Zhejiang University of Technology, 18#Chaowang Road, Hangzhou, Zhejiang 310014, PR China (F. Chen). Second Affiliated Hospital of Zhejiang University School of Medicine, Cardiovascular Key Lab of Zhejiang Province, 88#Jiefang Road, Hangzhou, Zhejiang 310009, PR China (Y. Xie and Z. Liu).
E-mail addresses: jacksonchen008@163.com (F. Chen), xieyao@zju.edu.cn (Y. Xie), lawson4001@zju.edu.cn (Z. Liu).
[1] Yazhi Zhu, Jian Shen and Zheng Gu contributed equally to this work.

https://doi.org/10.1016/j.cej.2019.02.045
Received 24 October 2018; Received in revised form 22 January 2019; Accepted 6 February 2019
Available online 11 February 2019
1385-8947/

to 9.22 MPa). Due to the incorporation of the PCL-derived copolymer, the material shows excellent affinity to cells, which is demonstrated by the cell proliferation and release of LDH. The hemolysis ratio of PCL-derived photocured materials is all < 5%, while the PEGDA photocured material is ~17%. It can also be observed that PCL-derived photocured material will improve the biocompatibility and reduce biotoxicity compared with PEGDA. This facile route for synthesis of biocompatible photocured resin with micrometer-resolute patterns has a good impact in bioengineering and biomedical fields.

1. Introduction

UV-curable rapid prototyping technology is a fast developing "green" technology. It has the advantages of high reaction efficiency, quick reaction speed, energy conservation and less organic volatile (VOC), thus photocurable polymers have a unique advantage in biomedical applications [1–6]. Resins used while fabricating scaffolds for tissue engineering require possessing good biocompatibility and high resolution structure [7–9]. Recently, micropatterned resins, as cell culture substrates or microactuators are gaining attentions in bioengineering [5,10]. UV irradiation is the facile fabrication of micropatterned resins by photolithography. For example [11–13], thiol-ene "click" reaction by UV irradiation could prepare micrometer-resolute hydrogel patterns with tailored architecture and multi-responsive properties.

However, most of the photocured resin involves large amounts of small molecules, such as photo-initiator, solvents and so on, which affect biological toxicity because of incomplete polymerization and organic residue [14–16]. Currently, there are abundant photocurable monomers [17–22] that have been developed and commonly been applied in bioengineering and biomedical fields. The photocurable monomers like poly(ethylene glycol) diacrylate (PEGDA), hyaluronic acid (HA) and their derivatives, dextran, and PEGDA [17,23,24] have relatively higher commercial value because of their low price and high product maturity. These are widely used as crossing agents to prepare hydrogels or photocurable resins. They have potential applications in the fields of neural prosthetic devices, biosensors and drug delivery [25–28]. Although the use of PEGDA has been relatively matured, there are still some unsolved problems. One of the problems is that PEGDA has poor toughness and ductility although it possesses strong mechanical properties. Another problem is that its biological toxicity is relatively high, that limits its further commercialization in the bioengineering [29,30].

Caprolactone (CL), another widely used monomer for injectable drug-delivery system, cell culture, etc., has a good biocompatibility and elasticity [31–34]. For example, Ai Ping Zhu's team have prepared a

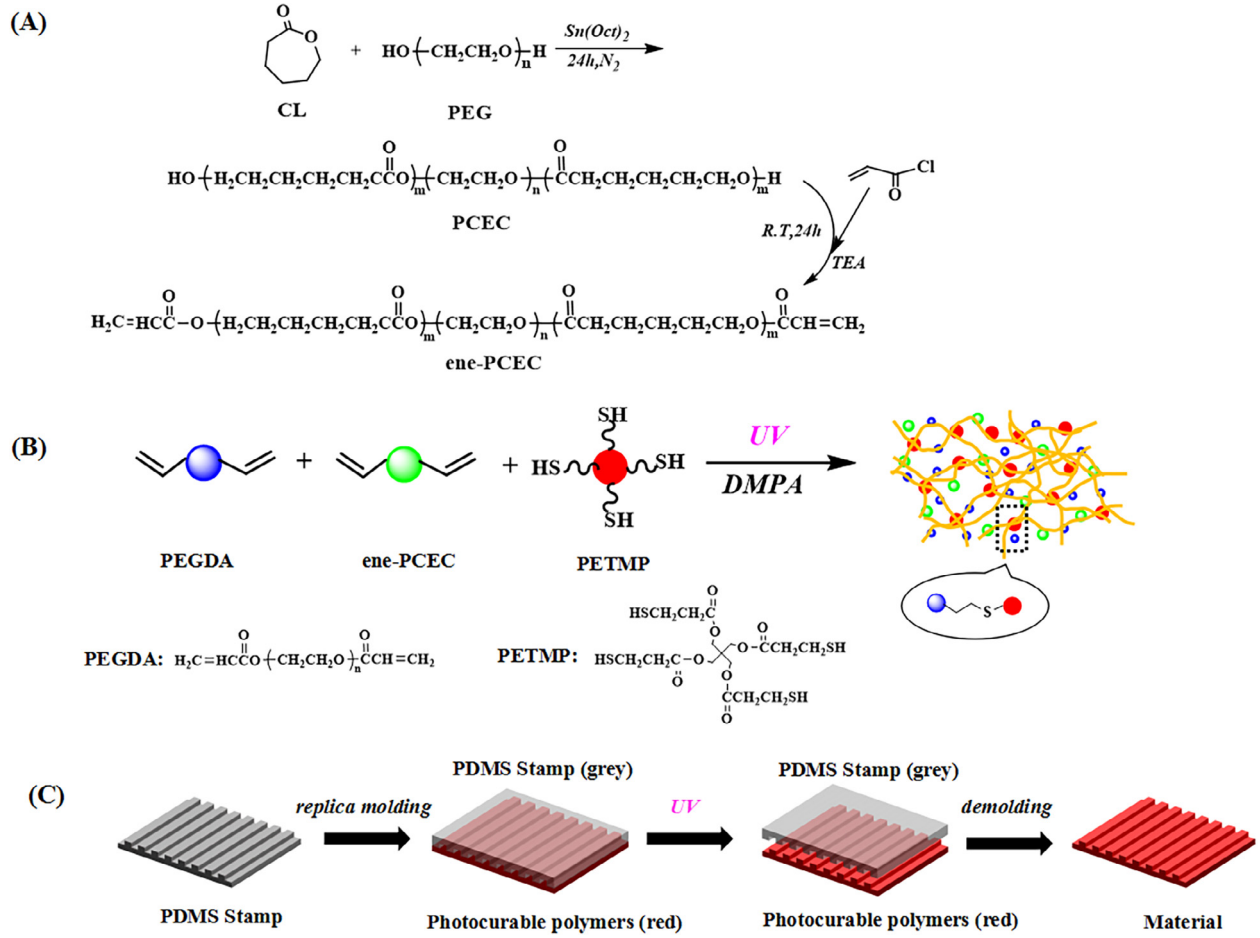

Scheme 1. Scheme illustrating the UV-crosslinking resin. (A) A synthesis procedure of the PCEC and ene-PCEC copolymers via ring-opening polymerization and substitution reaction respectively. (B) The curing process of photocured material via UV light in a simple diagrammatic form. (C) The fabrication process for the micropatterned samples, PDMS stamp, is in opaque grey and photocured sample is in solid red. (For interpretation of the references to colour in this figure legend, the reader is referred to the web version of this article.)

foldable micropatterned hydrogel film made from PCL-b-PEG-b-PCL-DA by UV embossing, and the hydrogel was found to have good biocompatibility compared with PEGDA hydrogel [35]. Therefore, the combination of caprolactone and PEGDA can not only improve the biotoxicity and degradation performance of PEGDA, but also have potential to produce high precision products by 3D printing technology [5]. For example, researchers were able to produce a high resolution (< 10 μm) tissue engineering scaffold by developing the structure of polycaprolactone-derived (PCL-derived) aliphatic copolymers initiated by two-photon polymerization (2PP). However, the device is very expensive and the rate of molding is slow. Therefore, it is urgent to develop a photocured material by UV rapid prototyping technology with high resolution, low cytotoxicity, and suitable mechanical properties [8,32].

Herein, our group provides a novel routine for the preparation of the photocured material with excellent biocompatibility and enhanced mechanical property. We discovered that with the incorporation of the photocurable PCL-derived copolymer into PEGDA resin, the biotoxicity and mechanical property of PEGDA could be improved. Scheme 1A shows a general procedure to prepare the photocurable PCL-derived copolymer. The precursor was cross-linked by thiol-ene "click" reaction (Scheme 1B). The mercaptan group was used as the crosslinking agent to enhance the mechanical properties of the material and reduce the residue of small molecular initiator [11,12,36]. The feed reactants were all liquid in this methodology, which enabled the reaction with no solvent. Besides, thiol-ene polymerization can be carried out under the mild condition, because the reaction is insensitive to environmental conditions and has high reaction efficiency. This method has the advantages of simplicity, versatility and has no risks of contamination. The performance of PCL-derived photocured material by UV-initiated thiol-ene "click" reaction was greatly improved: (1) The mechanical strength and toughness of the photocured materials was enhanced significantly; (2) "Click" chemistry gave it the advantage of high precision patterning; (3) The biocompatibility of the photocured materials was greatly improved.

2. Experimental

2.1. Materials

Poly(ethylene glycol) (PEG, Mn = 200), calcium hydride (CaH_2), caprolactone (CL), acryloyl chloride, poly(ethylene glycol) diacrylate (PEGDA), pentaerythritol tetra(3-mercaptopropionate) (PETMP), 2,2-dimethoxy-2-phenylacetophenone (DMPA) and stannous octoate (Sn $(Oct)_2$) were purchased from Aladdin Company (China). Toluene was purchased from Hangzhou Shuanglin Chemical Reagent Co., and ethanol was purchased from Zhejiang Hannuo Chemical Technology Co., Ltd.

2.2. Fabrication of PCL-derived photocured material

2.2.1. Synthesis of PCL/PEG/PCL(PCEC)

A biodegradable triblock polyetherester copolymer (PCL/PEG/PCL, PCEC) was synthesized by ring-opening polymerization. All reagents and solvents were pretreated with CaH_2 to remove water before the reaction. During the reaction, the reaction was protected by N_2. Caprolactone synthesization was initiated by the polymerization of PEG. Briefly, (0.400 g, 2 Mmol) PEG and (1.620 g, 4 Mmol) stannous octoate (PEG/stannous octoate = 1/2 M ratio) were dispersed in toluene and then reacted at room temperature for 15 min. Then (7.990 g, 0.07 mol) caprolactone was subsequently dissolved in the mixture at 90 °C for 24 h.

2.2.2. Synthesis of photocurable PCEC (ene-PCEC)

An ene-functionalized polymer was synthesized in two steps. Firstly, (2.5 Mmol) PCEC and (0.759 g, 7.5 Mmol) triethylamine were dissolved in (40 mL) dichloromethane. Secondly, an excess of acryloyl chloride (0.679 g, 7.5 Mmol) was slowly added to the mixture, and then the reaction is allowed to proceed for 24 h at room temperature. The final solution was dialyzed in $NaHCO_3$, HCl and NaCl solution (to remove the by-product). In the end, ene-PCEC was precipitated in ether.

2.2.3. Photopatterning process

The photopatterning process was prepared as following. A solution containing ene-PCEC, PEGDA, PETMP (the molar ratio of the functional vinyl and thiol groups was 1:1), and DMPA was dropped onto a template for 5 min while irradiating with a UV lamp (5 w, 365 nm). PEGDA/ene-PCEC's ratio of 25:1, 20:1, 15:1, 10:1 were used to prepare different photocured samples (as shown in Table 1).

The PDMS soft mold used in our study is obtained by a silicon mold. We can easily prepare it by casting PDMS on the surface of the silicon mold, then curing and removing PDMS from the silicon mold. Finally, the patterns can be repeated with the same accuracy as that on the silicon mold [11,37].

Table 1
The composition of photocured samples in this work.

Photocured Samples		PEGDA/ene-PCEC/PETMP (molar ratio)	$M_{n(PCEC)}$		ene-PCEC/Resin[c]		CL Segments/Resin[d]	
			Theories[a]	Calculated[b]	Molar Ratio (%)	Weight Ratio (wt.%)	Molar Ratio (%)	Weight Ratio (wt.%)
Control	Pure PEGDA	20/0/10	–	–	0	0	0	0
Series1	Series1-1	25/1/13	2480	1600	2.6	12.4	30.8	10.9
	Series1-2	20/1/10.5			3.2	14.9	38.4	13.0
	Series1-3	15/1/8			4.2	18.8	50.4	16.5
	Series1-4	10/1/5.5			6.1	25.4	73.2	22.2
Series2	Series2-1	25/1/13	3050	2400	2.6	17.5	49.4	15.3
	Series2-2	20/1/10.5			3.2	20.8	60.8	18.2
	Series2-3	15/1/8			4.2	25.8	79.8	22.6
	Series2-4	10/1/5.5			6.1	33.9	115.9	29.7
Series3	Series3-1	25/1/13	3620	3600	2.6	24.1	78.0	21.1
	Series3-2	20/1/10.5			3.2	28.3	96.0	24.8
	Series3-3	15/1/8			4.2	34.3	123.0	30.0
	Series3-4	10/1/5.5			6.1	43.4	183.0	38.0

[a] Was calculated by the molar ratio of monomers attend the copolymerization.
[b] Was calculated by ^1H NMR.
[c] Was calculated by the proportion of ene-PCEC in total resin.
[d] Was calculated by the proportion of PCL segments in total resin, based on $M_{CL}/(M_{ene\text{-}PCEC} + M_{PEGDA} + M_{PETMP})$.

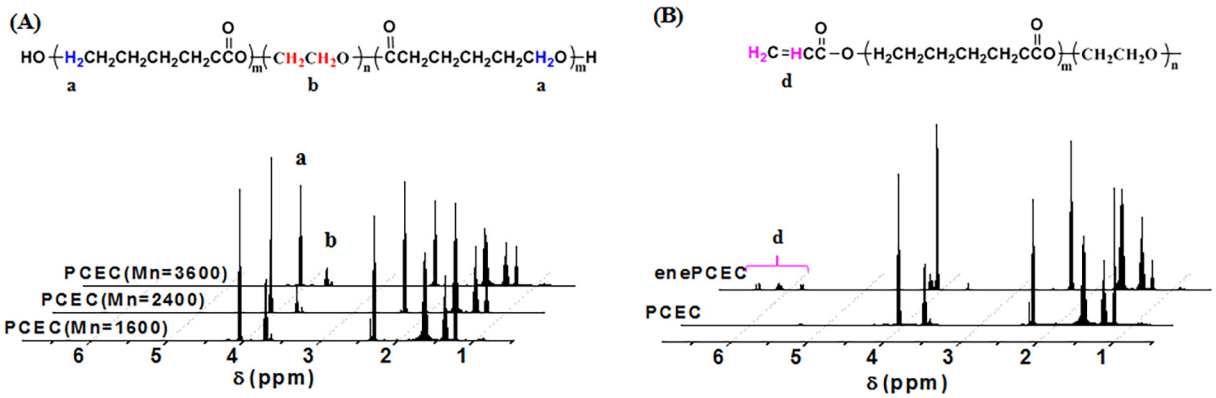

Fig. 1. (A) The ^{1}H NMR spectra of PCEC copolymers, the M_n of PCEC copolymer was 1600, 2400 and 3600, respectively. (B) The ^{1}H NMR spectra of PCEC and ene-PCEC copolymers.

Table 2
The molecular weights of a series of PCEC copolymers.

PCEC Copolymers	M_n		DP[a] (M_{CL}/M_{PEG})
	^{1}H NMR	GPC	
Series1	1600	–	12/1
Series2	2400	–	19/1
Series3	3600	4500	30/1

[a] The DP (degree of polymerization) was calculated by ^{1}H NMR.

Table 3
Thermal properties of photocured samples measured by DSC.

Photocured Samples		T_g (°C)	T_m (°C)	X_c (%)[a]
Control	Pure PEGDA	−28.12	–	–
Series1	Series1-1	−28.41	51.14	43.3
	Series1-2	−28.82	51.95	47.6
	Series1-3	−28.52	52.62	45.5
	Series1-4	−28.35	51.79	47.6
Series2	Series2-1	−29.07	53.45	52.1
	Series2-2	−28.57	54.47	46.4
	Series2-3	−30.88	53.93	48.9
	Series2-4	−31.07	55.10	46.9
Series3	Series3-1	−31.67	52.00	49.4
	Series3-2	−30.44	51.95	43.5
	Series3-3	−30.63	52.62	43.0
	Series3-4	−30.74	51.79	44.0

[a] The crystallinity (X_c) was calculated by Eq. (2).

2.3. Instruments and measurements

^{1}H Nuclear Magnetic Resonance (^{1}H NMR) was performed using an AVANCE 500 MHz instrument (Bruker company) and deuterochloroform solvent. Differential scanning calorimetry (DSC) test was performed with a DSC1 STAR^e System. The experiment was carried out between −60 °C and 80 °C with a heating rate of 10 °C/min. Dynamic thermomechanical analysis (DMA, American TA Q800) was carried out between −100 °C and 60 °C with a heating rate of 3 °C/min, a frequency of 1 Hz and an amplitude 15 μm. Tensile test was performed using a universal US Instron machine. Water absorption property was expressed by comparing different rates of increase in mass of the material after enough absorption.

2.4. Cell culture

The HUVECs, VSMCs, and L929 cell line were obtained from the Institute of Biochemistry and Cell Biology, Chinese Academy of Science. The cells were cultured in DMEM supplemented with 1.5 g/L sodium bicarbonate, 10% fetal bovine serum, 100 U/mL penicillin, and 100 μg/mL streptomycin at 37 °C in a humidified atmosphere of 5% CO_2. Cells were fed every 3 days, and sub-cultured at 70–80% confluency.

2.5. Cell proliferation assay

An MTS cell proliferation assay was performed according to the manufacturer's protocol (ab197010, Abcam). Briefly, L929 cells were seeded into 96-well plates and subjected to serum deprivation for 24 h. Then the extraction of PEDGA or PCL was used to stimulate the L929 cells for another 24 h. Finally, cells were incubated with MTS solution for 4 h. The absorbance was measured using spectrophotometer [38].

2.6. Lactate dehydrogenase (LDH) – cytotoxicity assay

Cell death or cytotoxicity is classically evaluated by the quantification of plasma membrane damage. Unlike other cytoplasmic enzymes that are unstable or exist in low amount in most of the cells, LDH is a stable cytoplasmic enzyme present in all cells and rapidly released into the cell culture supernatant upon damage of the plasma membrane. In

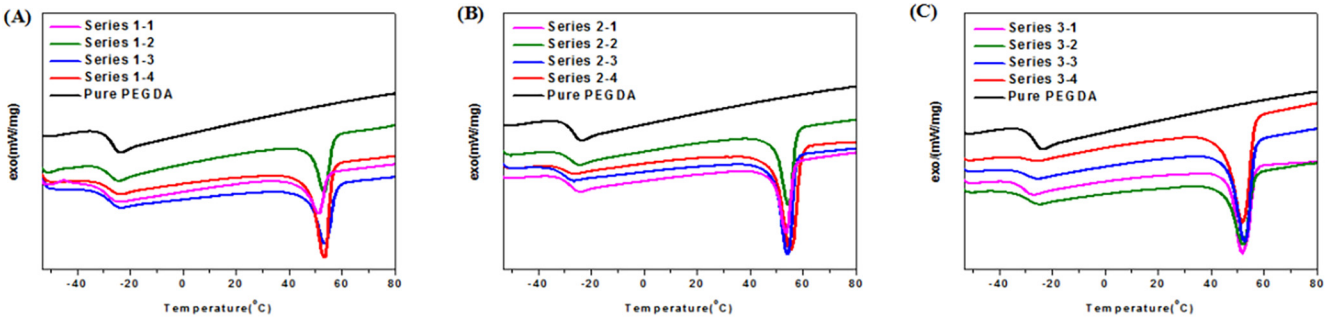

Fig. 2. The DSC curves of the photocured samples. (A-C) $M_{n(PCEC)}$ was 1600, 2400 and 3600, respectively.

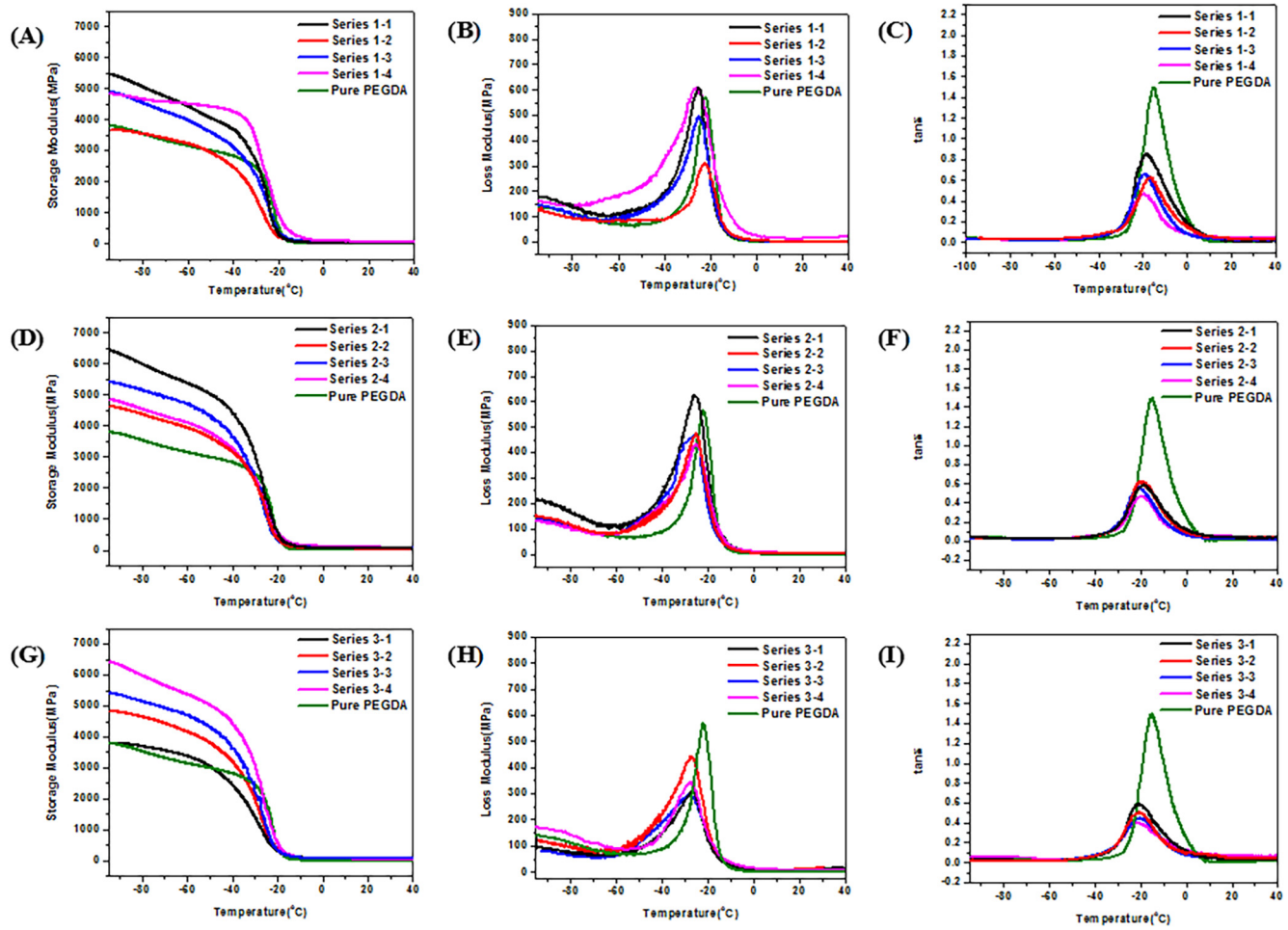

Fig. 3. The DMA results of the photocured samples. (A-C) The storage modulus (E'), loss modulus (E''), and loss factor (tan δ) of the photocured samples respectively, $M_{n(PCEC)}$ = 1600. (D-F) The storage modulus (E'), loss modulus (E''), and loss factor (tan δ) of the photocured samples respectively, $M_{n(PCEC)}$ = 2400. (G-I) The storage modulus (E'), loss modulus (E''), and loss factor (tan δ) of the photocured samples respectively, $M_{n(PCEC)}$ = 3600.

Table 4
The mechanical properties of photocured samples (E', peak temperature of E'' and peak temperature of tan δ were measured by DMA; Breaking strength, Young's modulus and elongation at break were measured by tensile test).

Photocured Samples		E' (MPa)		Peak Temperature of E'' (°C)	Peak Temperature of tan δ (°C)	Breaking Strength (MPa)	Young's Modulus (MPa)	Elongation at Break (%)
		at −40 °C	at 37 °C					
Control	Pure PEGDA	2825.3	2.3	−21.8	−15.2	0.62	1.39	46.64
Series1	Series1-1	3669.5	12.2	−25.2	−18.2	0.81	1.85	58.23
	Series1-2	2461.0	23.1	−22.4	−17.2	1.09	2.07	66.56
	Series1-3	3132.3	50.2	−24.9	−19.8	1.16	4.00	56.65
	Series1-4	4025.2	69.9	−26.7	−19.9	1.45	4.50	43.32
Series2	Series2-1	4420.6	45.5	−25.9	−19.9	0.84	2.39	56.08
	Series2-2	3170.5	32.3	−25.4	−19.5	0.95	3.65	48.21
	Series2-3	3658.3	83.5	−27.0	−20.2	1.34	6.43	50.48
	Series2-4	3259.0	73.9	−24.7	−19.6	2.13	9.72	45.75
Series3	Series3-1	4416.7	45.7	−26.7	−20.6	1.67	4.58	54.97
	Series3-2	3202.4	46.5	−27.4	−20.8	2.11	6.90	58.31
	Series3-3	3650.3	82.4	−27.4	−21.0	2.49	7.66	48.32
	Series3-4	2446.6	48.5	−27.5	−21.3	3.10	9.22	51.66

our study, LDH release was measured with a cytotoxicity kit assay (ab65391, Abcam) on the basis of the cleavage of a tetrazolium salt by LDH [39]. L929 cells were seeded into 96-well plates and exposed to the extractions of PEDGA or PCL for 24, 48, and 72 h. 100 μL of culture medium was collected, centrifuged to remove cellular debris, and transferred to a 96-well plate. 100 μL of the reaction mixture was added to each well and incubated for 30 min at room temperature [40]. Absorbance was measured at 490 nm, and LDH release was expressed as a percentage of total LDH activity, measured by lysing cells with Triton X-100.

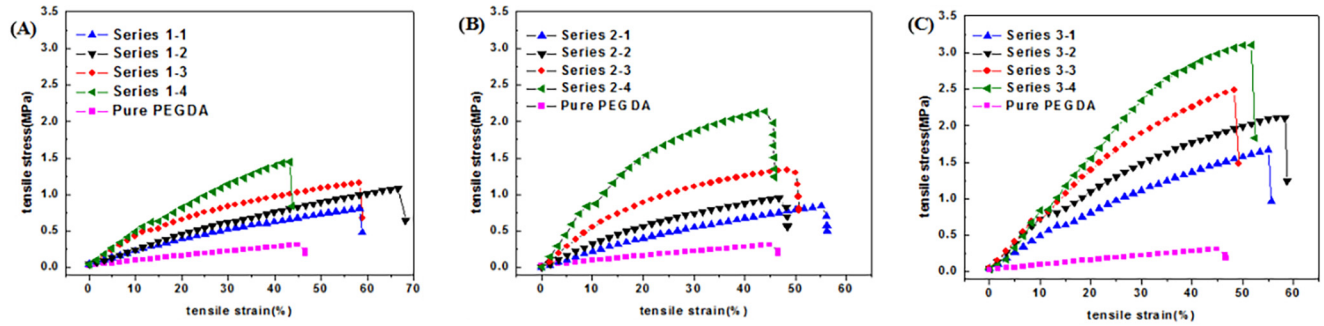

Fig. 4. The stress-strain curves of the photocured samples. (A-C) $M_{n(PCEC)}$ was 1600, 2400 and 3600, respectively.

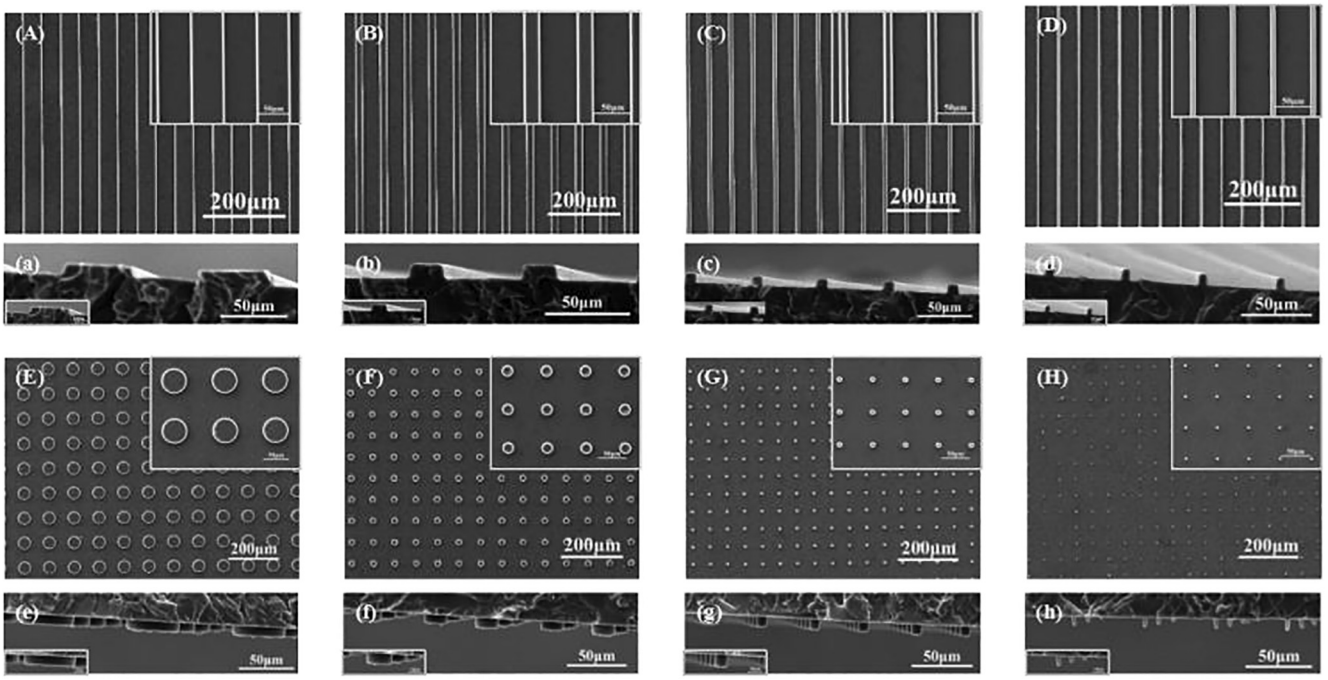

Fig. 5. Scanning electron microscope images of the surface and cross sections of the micropatterned materials. The composition of photocured samples was prepared from the sample Series3-4. Images (A-D) were ridge/groove micropatterns. The height of a ridge was 10 μm, and the widths were 50 μm, 20 μm, 10 μm and 5 μm, respectively. Images (E-H) were cylindrical array micropatterns. The height of cylinder was 10 μm, and the diameters were 50 μm, 20 μm, 10 μm and 5 μm, respectively. The last row images (e-h) were the cross sections corresponding to the different micropatterns.

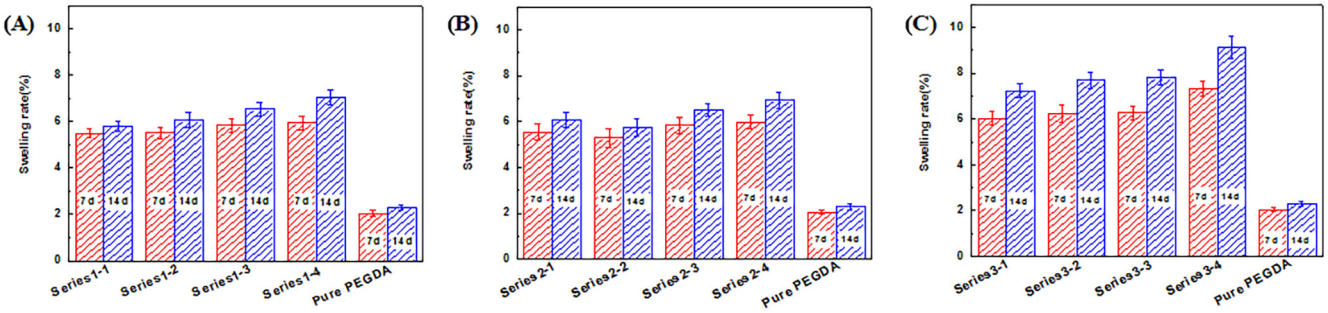

Fig. 6. Water absorption of photocured materials. (A-C) $M_{n(PCEC)}$ was 1600, 2400 and 3600, respectively. Red indicates that the resin was immersed in deionized water for 7 days; blue indicates that the resin was immersed in deionized water for 14 days. (For interpretation of the references to colour in this figure legend, the reader is referred to the web version of this article.)

2.7. Hemolysis test

According to ISO 10993-4: 2017, 100 mg of PCL or PEDGA test piece was soaked in 1 mL phosphate-buffered saline (PBS) (test group) for 48 h, 1 mL distilled water (positive control group) or 1 mL normal PBS (negative control group) (https://www.iso.org/standard/63448.html). Six paralleled samples were laid in each group. All tubes were put into the 37 °C thermostatic water bath case for 30 min. 0.8 mL arterial blood of a healthy adult New Zealand albino rabbit was immediately mixed with 1 mL normal PBS which contained 0.01 g/L

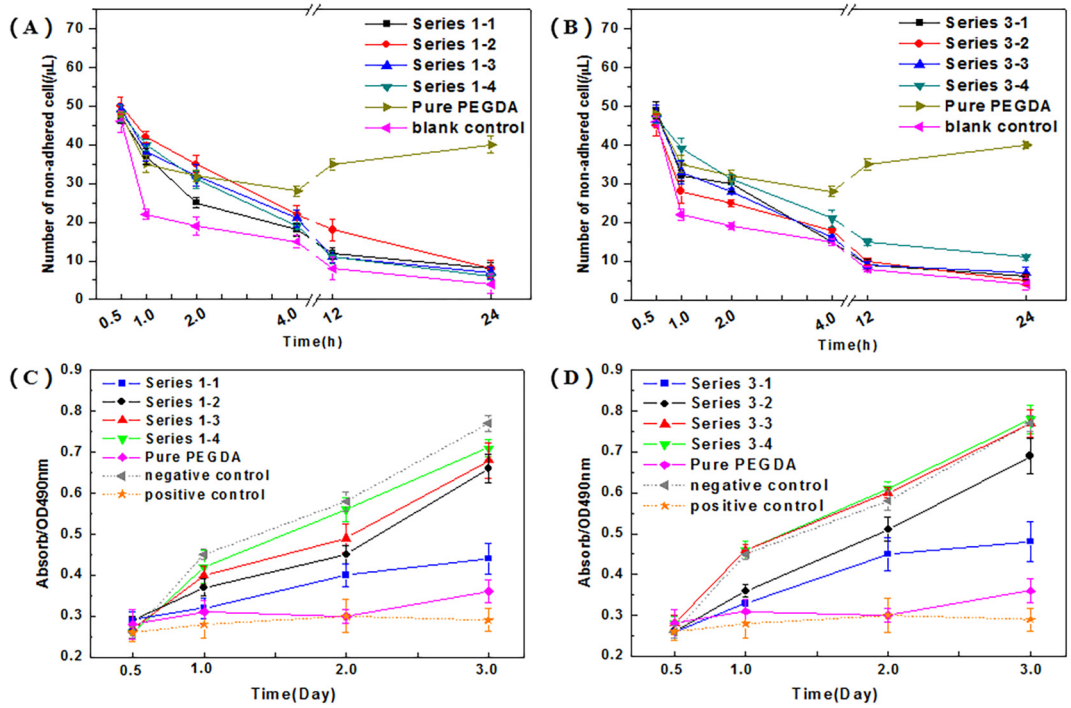

Fig. 7. Cell adhesion and viability of L929 fibroblasts on the surface of pure PEDGA and PCL-derived material. (A-B) Numbers of non-adhered cells on the surface of materials. (C-D) Cell viability measured by MTS reduction of L929 cell line.

Table 5
The cell viability of photocured samples.

Photocured Samples		Cell Viability (%)[a]			
		0.5 Day	1.0 Day	2.0 Day	3.0 Day
Positive Control	0.64% Phenol Culture	100.0	62.2	51.7	37.7
Control	Pure PEGDA	107.7	68.9	51.7	46.8
Series 1	Series 1-1	100.0	71.1	69	57.1
	Series 1-2	103.8	82.2	77.6	85.7
	Series 1-3	111.5	88.9	84.5	88.3
	Series 1-4	111.5	93.3	96.6	92.2
Series 2	Series 2-1	100.0	73.3	77.6	62.3
	Series 2-2	100.0	80.0	879	89.6
	Series 2-3	107.7	102.2	103.4	100.0
	Series 2-4	107.7	102.2	105.2	101.3

[a] Was measured by MTS cell proliferation assay and was calculated by using the following Eq. (3) [44].

potassium oxalate decoagulant, in this way, the fresh anticoagulant diluted cony blood was prepared. Then 0.2 mL of diluted blood was added to each tube. All the test tubes were put into the 37 °C thermostatic water bath for 60 min and centrifuged at 2500 rpm for 10 min. The A value was evaluated by a spectrophotometer at 545 nm wavelength. The mean value of the six samples was calculated as a group A value. According to ISO 10993-4: 2002, the hemolytic ratio was calculated according to the following: hemolysis radio (%) = $[(OD_{exp} - OD_{con\text{-}neg})/(OD_{con\text{-}pos} - OD_{con\text{-}neg})]$*100%. The measured optical density (OD) values of the experimental, negative control and positive control groups were coded as OD_{exp}, $OD_{con\text{-}neg}$, $OD_{con\text{-}pos}$, respectively.

2.8. Scanning electron microscope (SEM)

SEM was used to detect the morphology of HUVECs, VSMCs, and L929 cells. In brief, the specimens were fixed with 2.5% glutaraldehyde for > 4 h. After washing three times with PBS, the specimens were post-fixed with 1% OsO_4 for 1–2 h. Next, the specimens were dehydrated by an ethanol gradient, followed by acetone for overnight infiltration. Furthermore, the specimens were embedded in Spurr resin and sectioned in the Leica EM UC7 Manufacturer (Leica, Wetzlar, Germany) [41]. The sections were stained with uranyl acetate and alkaline lead citrate, and the images were procured randomly by Hitachi Model H-7650 SEM.

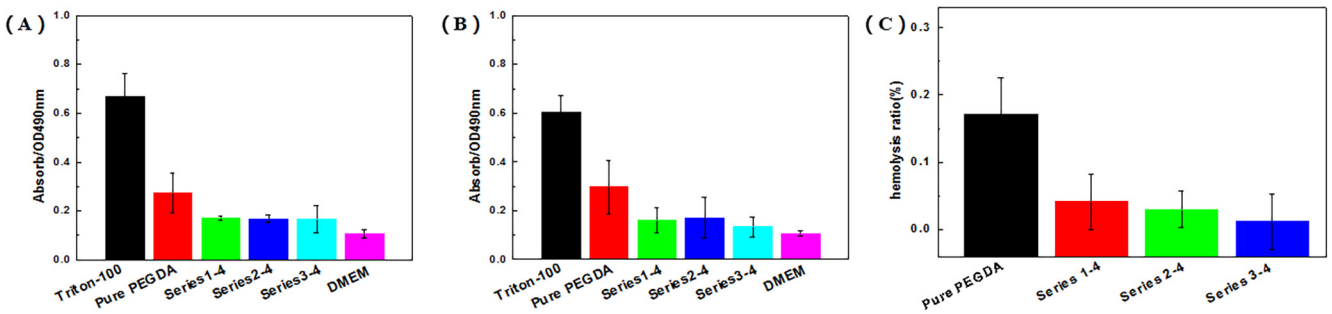

Fig. 8. LDH release and hemolysis test results of the photocured materials. (A-B) LDH releases of the photocured materials, L929 cells were stimulated with the extractions of PEDGA and PCL for 24 and 48 h. (C) Hemolysis ratio of the photocured materials with the extractions of PEDGA and PCL for 48 h.

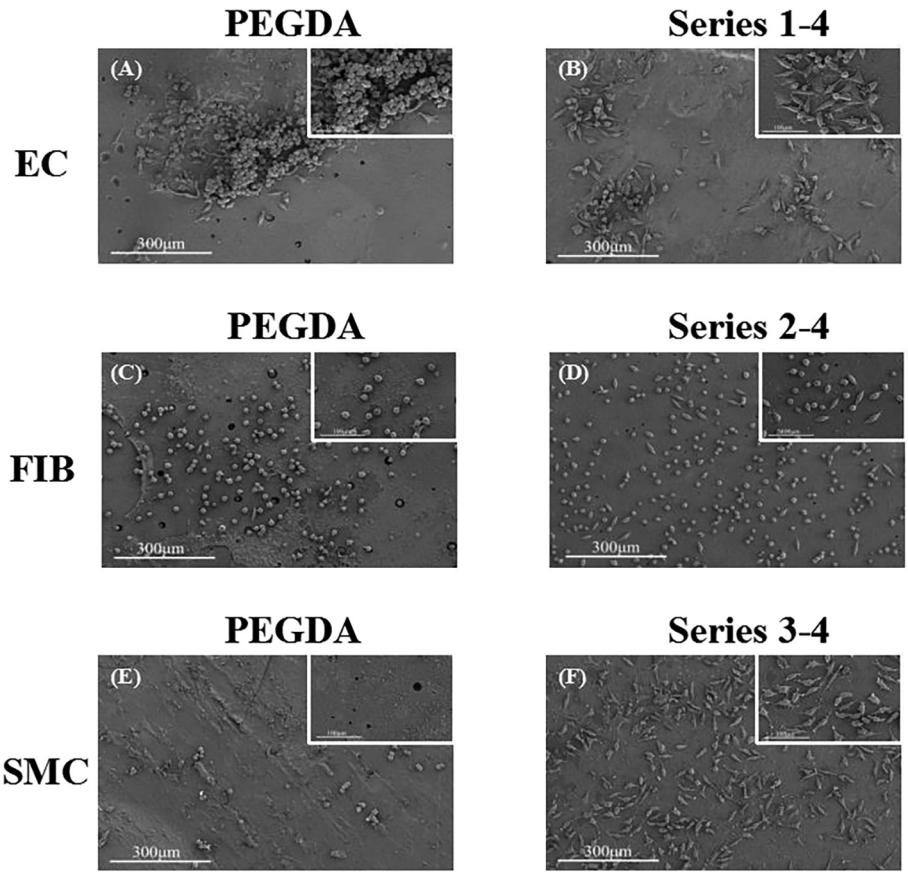

Fig. 9. The morphology of the photocured materials to ECs (A-B), SMCs (C-D), and FBs (E-F) measured by SEM.

2.9. Statistical analysis

All data are presented as the Mean ± SD. Two-tailed Student's *t*-tests were performed to compare means of two groups. ANOVA followed by Bonferroni's multiple comparisons was used to compare means from three or more groups. A p-value of less than 0.05 was considered to be statistically significant.

3. Results and discussion

3.1. Synthesis and characteristic of precursor

As shown in Scheme 1A, a controlled ring-opening polymerization initiated by the hydroxyl group of the PEG molecule under the existence of $Sn(Oct)_2$ could be obtained by controlling the content of PCL and the time of polymerization [33]. To confirm the formation of PCEC and ene-PCEC copolymers, ^{1}H NMR was performed and the results were shown in Fig. 1. In Fig. 1A, peaks at the chemical shifts of 3.72 ppm and 4.06 ppm were assigned to methylene protons of $-CH_2CH_2O-$ in PEG units and $-COOCH_2-$ in PCL units, respectively [33,42]. In Fig. 1B, compared with PCEC copolymer, ene-PCEC copolymer showed a peak at ~6 ppm, which was attributed to vinyl protons of $CH_2{=}CH-$ at the end-acrylate groups, indicating successful preparation of ene-PCEC copolymer. The molecular weight of PCEC copolymers was calculated from ^{1}H NMR according to Eq. (1) and the results were listed in Table 2. GPC test was also used to further characterize the molecular weight of PCEC copolymer in Table 2.

$$\boldsymbol{M_{n(PCEC)}} = \left(\frac{S_a}{S_b} \times \boldsymbol{M_{n(PEG)}} \times \boldsymbol{M_{n(CL)}}\right)\Big/_{44} + \boldsymbol{M_{n(PEG)}} \quad (1)$$

where S_a, S_b were integral intensities of methylene protons of $-OCH_2CH_2-$ in PEG unit at 3.72 ppm and methylene protons of $-COOCH_2-$ in PCL units at 4.06 ppm, respectively. $M_{n(PCEC)}$, $M_{n(PEG)}$ and $M_{n(CL)}$ represented the molecular weight of PCEC, PEG and CL.

3.2. Synthesis and characteristics of photocured materials

As shown in Scheme 1B, the obtained ene-PCEC copolymer was dissolved well in the PEGDA and was cross-linked through a photopolymerization under UV irradiation [36]. This method was facile and efficient, which could improve the conversion rate of products as well as the thermal and mechanical properties of PEGDA photocured material. The thermal property of the photocured materials was measured by DSC. As shown in Fig. 2, both PCL-derived photocured samples and pure PEGDA photocured samples showed a glass transition temperature (T_g) induced by PEG, but the T_g of PCL-derived photocured samples was slightly lower than that of PEGDA photocured samples. Interestingly, it is seen in Table 3 that as the molecular weight of ene-PCEC increases (from Series 1 to Series 3), the T_g of photocured materials decreases. With the increase of molecular weight, the regularity of crosslinking network was destroyed and the flexibility of photocured materials was improved. Besides, there was a melting peak (T_m) corresponding to PCL in the PCL-derived photocured samples while pure PEGDA photocured sample did not show any T_m. As summarized in Table 3, the degree of crystallinity (X_c) of PCL-derived photocured samples is around 50%, which is lower than that of the pure precursors (as shown in Fig. S1 and Table S1). The reason for the lower degree of crystallinity of PCL-derived photocured samples might be that the crosslinking network prevented crystallization of partial PCL segments, which decreased the crystallization and improved the flexibility of PCL chains. This can be further proved from its mechanical property.

$$X_c = \Delta H_m/\Delta H_{m,c} \times 100\% \quad (2)$$

where ΔH_m was measured by DSC, $\Delta H_{m,c}$ was theoretical melting

enthalpy of 100% crystallization, and $\Delta H_{m,c}$ (PCL) = 139.5 J/g [43].

For biomedical materials, the mechanical property was one of the most important factors that influence their application fields and performance. Here, the dynamic mechanical property was measured by DMA. Fig. 3A-I showed the storage modulus (E'), loss modulus (E'') and loss factor (tan δ), respectively. In Fig. 3, PCL-derived photocured samples showed better E' than that of the pure PEGDA photocured sample. In Table 4 the details of the photocured materials were further analyzed. At −40 °C (below T_g), the E' of the PCL-derived photocured samples was higher than that of pure PEGDA photocured samples. This feature was even more obvious at 37 °C (near the body temperature), which indicated that the strength of the PCL-derived photocured samples at body temperature was much better than that of the pure PEGDA photocured sample. Meanwhile, PCL-derived photocured samples showed better E'' and loss factor (tan δ). The tan δ of pure PEGDA photocured sample was higher than the PCL-derived photocured samples, which meant that the mechanical property of pure PEGDA photocured sample was poor at low temperature. That was also confirmed by the peak temperature of E'' and tan δ in Table 4. When the PCL segments were incorporated into the network, both the peak temperature of E'' (from −21.8 °C to −27.5 °C) and tan δ (from −15.2 °C to −21.3 °C) decreased which suggested that the flexibility and toughness of the PCL-derived photocured samples were improved. Moreover, with the increase in the molecular weight of ene-PCEC, the peak temperature of E'' and tan δ decreased. The results from the DMA test were consistent with the data of DSC (Table 3) and the DMA results were more sensitive to the thermal property of photocured materials. Among three factors (E', E'' and tan δ) examined, the incorporation of PCL segments into the cross-linked network was an effective way to enhance the flexibility and toughness of the PEGDA resin.

We further conducted a tensile test to examine the mechanical property of photocured samples. In Fig. 4A-C, the tensile strength of the PCL-derived photocured samples was obviously higher than that of the pure PEGDA photocured sample. The strength of the sample increased regularly as the content of PCL segments increased. And with the increase in the molecular weight of ene-PCEC, the tensile strength was further enhanced. This conclusion was also proved by the breaking strength and Young modulus in Table 4. In the case of Series3, with the increase of ene-PCEC content from 0 to 6.1 mol%, the breaking strength of the photocured samples monotonically increased from 0.62 to 3.10 MPa, and Young's modulus from 1.39 to 9.22 MPa. For elongation at break, the PCL-derived photocured samples increased slightly compared with the pure PEGDA photocured samples. Similar trends were observed in the case of Series1 and Series2. Obviously, incorporation of PCL segments into the cross-linked network can significantly improve the mechanical strength and toughness of PEGDA resin.

3.3. Photopatterning property

To explore the application of photocured material in bioengineering and biomedicine fields, the soft lithography techniques to perform microphotopatterning were used. Soft lithography techniques were based on in situ polymerization of precursor monomer solutions against microstructure stamps, which were then removed by demolding [5,11]. UV irradiation made the fabrication of patterns more facile. Fig. 5 showed that the patterns with various shapes and size could easily be fabricated. In our work, a precursor and a cross-linker were poured onto the PDMS mold and after 2 min of UV irradiation, the photocured sample was demolded from the PDMS mold to obtain a micropatterned sample (Scheme 1C). There were two examples of photopatterning (the patterning corresponding to a negative PDMS mold) taken by SEM. Hereon, sample Serial3-4 was chosen for exploring the precision of UV-initiated photopatterning in comparison with PEGDA. As Fig. 5A-H showed, different patterns of 5–50 μm precision were accurately reproduced. Unlike the pure PEGDA photocured samples (as shown in Fig. S2), PCL-derived photocured samples retained the characteristic of high precision. Fig. 6 showed the water absorption property of photocured samples. The water absorption of the PCL-derived photocured samples slightly increased and the crosslinking degree of photocured samples reached more than 90%. That was because the large molecular chain reduced the density of cross-linked network. The high-resolution patterning and low water absorption of our photocured samples provided a good basis for the application in bioengineering and biomedicine fields.

3.4. Biocompatibility

The biocompatibility of the polycaprolactone-derived photocured resin was investigated by testing the cell attachment and cell viability on different photopolymers. Interestingly, various degrees of cell adhesion and viability of L929 fibroblasts were observed on the surface of pure PEDGA and PCL material. Although the PEDGA group performance prevented cell attachment, the number of un-adhered L929 cells gradually declined in all PCL groups during the first 24 h, which indicated that PCL were apt to cell-seeding (Fig. 7A-B). MTS [3-(4,5-dimethylthiazol-2-yl)-5-(3-carboxymethoxyphenyl)-2-(4-sulfophenyl)-2H-tetrazolium] assay was used as a colorimetric method for determining the number of viable cells in proliferation. It was observed that the PCL protected the viability and proliferation ability compared with the pure PEDGA group (Fig. 7C-D). Absorbance in OD490 nm showed twice as many viable cells in PCL groups than in PEDGA group (~85% vs. ~40%) after 72 h (Table 5). Additionally, we reported that increasing the PCL content was beneficial for biocompatibility: Comparing the cell survival rates of series 1 and series 2, it was found that the cell survival rate has a positive link with increasing the molecular weight of ene-PCEC. Therefore, we concluded that higher PCL content would promote cell attachment and proliferation. As a result, we chose series 1–4, 2–4, and 3–4 in the following experiments. Additionally, L929 cells were stimulated with the extractions of PEDGA and PCL for 24 (Fig. 8A), 48 (Fig. 8B), and 72 h (Fig. S3), and media LDH concentration was tested. Data showed that the PCL extraction significantly reduced LDH release than PEGDA group extraction, which indicated PCL polymerization reduced the cytotoxicity of PEGDA (Fig. 8A-B). Hemolysis test also revealed that PCL protected the membrane integrity of erythrocytes with the increase of PCEC molecular weight (Fig. 8C).

Furthermore, normal cell morphology and a confluent cell sheet covering the surface was found with the help of scanning electron microscope (SEM) in the case of PCL, which confirmed the innocuousness of PCL to ECs, SMCs, and FBs (Fig. 9). However, the seeded cells on pure PEGDA were of paromorphia and disordered, indicating that PEGDA had a strong inhibitory effect on cell attachment. This result coincided with our previous studies on cell-repellency of PEGDA. These data proved that PCL could effectively improve the cell attachment of PEGDA. Additionally, the cell attachment was substantially influenced by the ratio of the PCL and PEGDA. Variation in cellular behavior was observed. L929 cells adhered and grew better on the scaffolds with the higher percentage of PCL content (Fig. 9).

$$\text{Cell Viability (\%)} = (OD_{exp} - OD_{bla})/OD_{bla} \quad (3)$$

where OD_{exp} and OD_{bla} was the OD values of the blank and experimental groups.

4. Conclusions

In a summary, a facile method for the preparation of photocured material with excellent biocompatibility and enhanced mechanical property was demonstrated. It consisted cross-linked and micropatterned photocurable polymers through thiol-ene "click" chemistry via UV irradiation, without adding initiators. In this work, the control of the photocured material's mechanical property and cell behavior depended on the content of PCL segment and the molecular weight of ene-PCEC copolymer. The main mechanical characterization of the

PCL-derived photocured material was measured with the help of tensile test. We demonstrated that with the increase of PCL segment content from 0 to 38.0%, the photocured samples monotonically increased their breaking strength from 0.62 to 3.10 MPa and Young's modulus from 1.39 to 9.22 MPa. The biocompatibility property measured by MTS assays and LDH release indicated that the cell viability of PCL-derived photocured materials has been significantly improved. The hemolysis ratio of all PCL-derived photocured materials is < 5%, while that of the PEGDA photocured material is ~17%. The morphology of photocured materials to ECs, SMCs, and FBs, measured by SEM showed excellent biocompatibility of PCL –derived photocured materials. In addition, the main novelty of this technique is the facile fabrication of high-resolution patterns (~5 μm) by photolithography. This novel routine for the fabrication of photocured material has potentials in finding wide applications in bioengineering and biomedical fields. The material can be used as scaffolds for the tissue engineering as well as substrates for cell culture.

Acknowledgements

This study was funded by the Natural Science Foundation of China (Nos. 81670433 and 81300236), the Natural Science Foundation of Zhejiang Province (Nos. LY16E030012, LY17E030006, LY18E030009 and LY19E030007), the Medical Scientific Research Foundation of Zhejiang Province (2016KYA097) and the Xin Miao Talent Program of Zhejiang Province (No. 2018R403052).

Appendix A. Supplementary data

Supplementary data to this article can be found online at https://doi.org/10.1016/j.cej.2019.02.045.

References

[1] Borsen Chiou, Srinivasa R. Raghavan, Saad A. Khan, Effect of colloidal fillers on the cross-linking of a UV-curable polymer: Gel point rheology and the Winter–Chambon criterion, Macromolecules 34 (2001) 4526–4533.
[2] R. Liu, X. Zhang, J. Zhu, X. Liu, Z. Wang, J. Yan, UV-curable coatings from multi-armed cardanol-based acrylate oligomers, ACS Sustainable Chem. Eng. 3 (2015) 1313–1320.
[3] F.A. Landis, J.S. Stephens, J.A. Cooper, M.T. Cicerone, L.G. Sheng, Tissue engineering scaffolds based on photocured dimethacrylate polymers for in vitro optical imaging, Biomacromolecules 7 (2006) 1751–1757.
[4] Q. Xu, A. Sigen, P. McMichael, J. Creagh-Flynn, D. Zhou, Y. Gao, X. Li, X. Wang, W. Wang, Double-cross-linked hydrogel strengthened by UV irradiation from a hyperbranched PEG-based trifunctional polymer, ACS Macro Lett. 7 (2018) 509–513.
[5] Y.S. Kim, N.Y. Lee, R.L. Ju, M. Jung Lee, S. Park, Nanofeature-patterned polymer mold fabrication toward precisely defined nanostructure replication, Chem. Mater. 17 (2005) 5867–5870.
[6] H. Chen, F. Yang, Q. Chen, J. Zheng, A novel design of multi-mechanoresponsive and mechanically strong hydrogels, Adv. Mater. 29 (2017) 1606900.
[7] Marga C. Lensen, Petra Mela, Ahmed Mourran, Jürgen Groll, Jean Heuts, A. Haitao Rong, Martin Möller, Micro- and nanopatterned star poly(ethylene glycol) (PEG) materials prepared by UV-based imprint lithography, Langmuir ACS J. Surfaces Colloids 23 (2007) 7841–7846.
[8] K.W. Lee, S. Wang, B.C. Fox, E.L. Ritman, M.J. Yaszemski, L. Lu, Poly(propylene fumarate) bone tissue engineering scaffold fabrication using stereolithography: effects of resin formulations and laser parameters, Biomacromolecules 8 (2007) 1077–1084.
[9] A. Sigen, Q. Xu, D. Zhou, Y. Gao, J.M. Vasquez, U. Greiser, W. Wang, W. Liu, W. Wang, Hyperbranched PEG-based multi-NHS polymer and bioconjugation with BSA, Polymer Chem. 8 (2017) 1283–1287.
[10] B. Chollet, M. Li, E. Martwong, B. Bresson, C. Fretigny, P. Tabeling, Y. Tran, Multiscale surface-attached hydrogel thin films with tailored architecture, ACS Appl. Mater. Interfaces 8 (2016) 11729.
[11] B. Chollet, L. D'Eramo, E. Martwong, M. Li, J. Macron, T.Q. Mai, P. Tabeling, Y. Tran, Tailoring patterns of surface-attached multi-responsive polymer networks, ACS Appl. Mater. Interfaces 8 (2017) 24870–24879.
[12] T.O. Machado, C. Sayer, P.H.H. Araujo, Thiol-ene polymerisation: a promising technique to obtain novel biomaterials, Eur. Polymer J. (2016) 200–215.
[13] L. Chang, F. Chen, X. Zhang, T. Kuang, M. Li, J. Hu, J. Shi, L.J. Lee, H. Cheng, Y. Li, Synthetic melanin E-ink, ACS Appl. Mater. Interfaces 9 (2017) 16553–16560.
[14] J. Wei, F. Liu, Novel highly efficient macrophotoinitiator comprising benzophenone, coinitiator amine, and thio moieties for photopolymerization, Macromolecules 42 (2009) 5486–5491.
[15] B. Gacal, H. Akat, D.K. Balta, N. Arsu, Y. Yagci, Synthesis and characterization of polymeric thioxanthone photoinitiators via double click reactions, Macromolecules 41 (2008) 2401–2405.
[16] C. Decker, C. Bianchi, S. Jönsson, Light-induced crosslinking polymerization of a novel-substituted bis-maleimide monomer, Polymer 45 (2004) 5803–5811.
[17] O. Kufelt, A. El-Tamer, C. Sehring, S. Schlie-Wolter, B.N. Chichkov, Hyaluronic acid based materials for scaffolding via two-photon polymerization, Biomacromolecules 15 (2014) 650–659.
[18] J. Decock, M. Schlenk, J.B. Salmon, In situ photo-patterning of pressure-resistant hydrogel membranes with controlled permeabilities in PEGDA microfluidic channels, Lab on A Chip 18 (2018).
[19] L. Ouyang, C.B. Highley, W. Sun, J.A. Burdick, A generalizable strategy for the 3D bioprinting of hydrogels from nonviscous photo-crosslinkable inks, Adv. Mater. 29 (2017) 1604983.
[20] L. Pescosolido, W. Schuurman, J. Malda, Hyaluronic acid and dextran-based semi-IPN hydrogels as biomaterials for bioprinting, Biomacromolecules 12 (2011) 1831–1838.
[21] S.Y. Choh, D. Cross, C. Wang, Facile synthesis and characterization of disulfide-cross-linked hyaluronic acid hydrogels for protein delivery and cell encapsulation, Biomacromolecules 12 (2011) 1126–1136.
[22] A. Berg, R. Wyrwa, J. Weisser, T. Weiss, R. Schade, G. Hildebrand, K. Liefeith, B. Schneider, R. Ellinger, M. Schnabelrauch, Synthesis of photopolymerizable hydrophilic macromers and evaluation of their applicability as reactive resin components for the fabrication of three-dimensionally structured hydrogel matrices by 2-photon-polymerization, Adv. Eng. Mater. 13 (2011) B274–B284.
[23] M. Bazzano, C. Barolo, R. Buscaino, G. D'Agostino, A. Ferri, M. Sangermano, R. Pisano, Controlled atmosphere in food packaging using ethylene–α-cyclodextrin inclusion complexes dispersed in photocured acrylic films, Ind. Eng. Chem. Res. 55 (2016) 579–585.
[24] H. Wang, J. Jasensky, N. Ulrich, J. Chen, H. Hao, C. Zhan, C. He, Capsaicin-inspired thiol–ene terpolymer networks designed for antibiofouling coatings, Langmuir 33 (2017) 13689–13698.
[25] J.L. Vanderhooft, B.K. Mann, G.D. Prestwich, Synthesis and characterization of novel thiol-reactive poly(ethylene glycol) cross-linkers for extracellular-matrix-mimetic biomaterials, Biomacromolecules 8 (2007) 2883–2889.
[26] Y. Xiao, L. He, J. Che, An effective approach for the fabrication of reinforced composite hydrogel engineered with SWNTs, polypyrrole and PEGDA hydrogel, J. Mater. Chem. 22 (2012) 8076–8082.
[27] H. Zhang, R. Shi, A. Xie, J. Li, L. Chen, P. Chen, S. Li, F. Huang, Y. Shen, Novel TiO_2/PEGDA hybrid hydrogel prepared in situ on tumor cells for effective photodynamic therapy, Appl. Mater. Interfaces 5 (2013) 12317–12322.
[28] P.J. Wu, J.L. Lilly, R. Arreaza, B.J. Berron, Hydrogel patches on live cells through surface mediated polymerization, Langmuir 33 (2017) 6778–6784.
[29] M.B. Browning, E. Cosgriffhernandez, Development of a biostable replacement for PEGDA hydrogels, Biomacromolecules 13 (2012) 779–786.
[30] L. Cai, J. Lu, V. Sheen, S. Wang, Promoting nerve cell functions on hydrogels grafted with poly(L-lysine), Biomacromolecules 13 (2012) 342–349.
[31] T. Weiß, R. Schade, T. Laube, A. Berg, G. Hildebrand, R. Wyrwa, M. Schnabelrauch, K. Liefeith, Two-photon polymerization of biocompatible photopolymers for microstructured 3D biointerfaces, Adv. Eng. Mater. 13 (2011) B264–B273.
[32] B.J. Green, K.S. Worthington, J.R. Thompson, S.J. Bunn, M. Rethwisch, E.E. Kaalberg, C. Jiao, L.A. Wiley, R.F. Mullins, E.M. Stone, E.H. Sohn, B.A. Tucker, C.A. Guymon, Effect of molecular weight and functionality on acrylated poly(caprolactone) for stereolithography and biomedical applications, Biomacromolecules 19 (2018) 3682–3692.
[33] C.B. Liu, C.Y. Gong, M.J. Huang, J.W. Wang, Y.F. Pan, Y.D. Zhang, G.Z. Li, M.L. Gou, K. Wang, M.J. Tu, Thermoreversible gel-sol behavior of biodegradable PCL-PEG-PCL triblock copolymer in aqueous solutions, J. Biomed. Mater. Res. Part B Appl. Biomater. 84B (2010) 165–175.
[34] D. Gräfe, A. Wickberg, M.M. Zieger, M. Wegener, E. Blasco, C. Barnerkowollik, Adding chemically selective subtraction to multi-material 3D additive manufacturing, Nature Commun. 9 (2018) 2788.
[35] A.P. Zhu, M.B. Chan-Park, J.X. Gao, Foldable micropatterned hydrogel film made from biocompatible PCL-b-PEG-b-PCL diacrylate by UV embossing, J. Biomed. Mater. Res. Part B: Appl. Biomater. 76B (2006) 76–84.
[36] B. Zhang, Z.A. Digby, J.A. Flum, P. Chakma, J.M. Saul, J.L. Sparks, D. Konkolewicz, Dynamic thiol-michael chemistry for thermoresponsive rehealable and malleable networks, Macromolecules 49 (2016) 6871–6878.
[37] D. Bartolo, G. Degré, P. Nghe, V. Studer, Microfluidic stickers, Lab on A Chip 8 (2008) 274–279.
[38] J. Shen, Y. Xie, Z. Liu, S. Zhang, Y. Wang, L. Jia, Y. Wang, Z. Cai, H. Ma, M. Xiang, Increased myocardial stiffness activates cardiac microvascular endothelial cell via VEGF paracrine signaling in cardiac hypertrophy, J. Mol. Cell. Cardiol. 122 (2018) 140–151.
[39] C. Spampanato, E. Feeney, L. Li, M. Cardone, J.A. Lim, F. Annunziata, H. Zare, R. Polishchuk, R. Puertollano, G. Parenti, Transcription factor EB (TFEB) is a new therapeutic target for Pompe disease, Embo Mol. Med. 5 (2013) 691–706.
[40] Y. Gouriou, P. Bijlenga, N. Demaurex, Mitochondrial Ca^{2+} uptake from plasma membrane Cav3.2 protein channels contributes to ischemic toxicity in PC12 cells, J. Biol. Chem. 288 (2013) 12459–12468.
[41] F. Yang, R. Wu, Z. Jiang, J. Chen, J. Nan, S. Su, N. Zhang, C. Wang, J. Zhao, C. Ni, Leptin increases mitochondrial OPA1 via GSK3-mediated OMA1 ubiquitination to enhance therapeutic effects of mesenchymal stem cell transplantation, Cell Death Disease 9 (2018) 556.
[42] S.Z. Fu, X.H. Wang, G. Guo, S. Shi, H. Liang, F. Luo, Y.Q. Wei, Z.Y. Qian,

Preparation and characterization of nano-hydroxyapatite/poly(ε-caprolactone)–poly(ethylene glycol)–poly(ε-caprolactone) composite fibers for tissue engineering, J. Phys. Chem. C 114 (2010) 18372–18378.
[43] C.G. Pitt, F.I. Chasalow, Y.M. Hibionada, D.M. Klimas, A. Schindler, Aliphatic polyesters. I. The degradation of poly(ϵ-caprolactone) in vivo, J. Appl. Polymer Sci. 26 (2010) 3779–3787.
[44] Y. Wang, B. Zhang, Z. Lin, Y. Li, F. Huang, S. Li, Y. Shen, A. Xie, Preparation and multiple antitumor properties of AuNRs/spinach extract/PEGDA composite hydrogel, ACS Appl. Mater. Interfaces 6 (2014) 15000–15006.